Journal of Cleaner Production 336 (2022) 130347

Contents lists available at ScienceDirect

Journal of Cleaner Production

journal homepage: www.elsevier.com/locate/jclepro

Model-based identification of the dominant N_2O emission pathway in a full-scale activated sludge system

Mojtaba Maktabifard [a,b,*], Kati Blomberg [c], Ewa Zaborowska [a], Anna Mikola [b], Jacek Mąkinia [a]

[a] Faculty of Civil and Environmental Engineering, Gdańsk University of Technology, Narutowicza Street 11/12, 80-233, Gdańsk, Poland
[b] Department of Built Environment, Aalto University, PO Box 15200, 00076, AALTO, Finland
[c] Helsinki Region Environmental Services HSY, PO Box 100, 00066, HSY, Finland

ARTICLE INFO

Handling Editor. Bin Chen

Keywords:
Wastewater treatment plant
Carbon footprint
Greenhouse gas emissions
Model calibration
Model application

ABSTRACT

Activated sludge models (ASMs), extended with an N_2O emission module, are powerful tools to describe the operation of full-scale wastewater treatment plants (WWTPs). Specifically, such models can investigate the most contributive N_2O production pathways and guide towards N_2O and carbon footprint (CF) mitigation measures. A common practice is to develop and validate models using data from a single WWTP. In this study, a successfully validated model in one plant (Slupsk/Poland) was extrapolated to another full-scale WWTP (Viikinmäki/Finland). For this purpose, the previously developed ASM No. 2d with the N_2O module was used. Moreover, the results of calibration and validation of that model were compared with those obtained on the basis of the ASM No. 3 with an N_2O module. A novel, rigorous calibration protocol, based on the system engineering approach, was implemented to minimize the number of adjusted parameters without compromising the accuracy of model predictions. The validated model accurately predicted the behavior of the system in terms of the liquid N_2O production in the bioreactor and gaseous N_2O emissions. Model-based identification of N_2O production pathways revealed the key role of heterotrophs duo to their high abundance in the microbial community. The N_2O emission factor (EF) at the studied plant was found between 0.9 and 0.94% of the influent TN-load for the validation and calibration period, respectively. Based on the model predictions, it was estimated that the aerobic zones contributed to over 93% of the N_2O emitted to the atmosphere, while the remaining portion (7%) resulted from the N_2O liquid-gas transfer in the non-aerated zones. The difference between the predicted N_2O EF and the empirical EF calculation would lead to almost 1000 tonnes of CO_2 equivalent reduction of the annual CF of the plant, which highlights the importance of model applications in CF studies.

1. Introduction

Traditionally, the operation of wastewater treatment plants (WWTPs) has solely been focused on efficient removing pollutants and nutrients from wastewater to protect public health and aquatic environment. More recently, new considerations have been postulated with respect to the energy efficiency and mitigation of greenhouse gas (GHG) emissions, which became important measures of the sustainability of WWTPs (Chen et al., 2020a).

Accumulated GHG emissions can be expressed as carbon footprint (CF) (Delre et al., 2019). Among the GHG emitted from WWTPs, nitrous oxide (N_2O) has received growing attention. It is estimated that the wastewater treatment sector is responsible for 3–5% of the global anthropogenic N_2O emission (Mannina et al., 2019). Furthermore, N_2O generated in wastewater treatment processes can dramatically affect the total CF of WWTPs. High shares, exceeding 50%, of N_2O emissions in CF of the biological nutrient removal (BNR) WWTPs have been reported in the literature (Koutsou et al., 2018).

It is challenging to determine precisely an N_2O emission factor (EF) (Sun et al., 2017). The empirical EFs are frequently reported based on the influent total nitrogen (TN) load, and the removed loads of TN or ammonium (NH_4^+-N). The choice of the EF may significantly affect the total calculated CF of WWTPs. High uncertainties in terms of CF have been shown when using the national GHG inventories approach (Nayeb et al., 2019).

Mechanistic activated sludge models (ASMs) are powerful tools to investigate the dominant N_2O production pathways and guide towards mitigation measures. Although modelling studies are a favorable

* Corresponding author. Faculty of Civil and Environmental Engineering, Gdańsk University of Technology, Narutowicza Street 11/12, 80, Gdańsk, Poland.
E-mail address: mojmakta@pg.edu.pl (M. Maktabifard).

https://doi.org/10.1016/j.jclepro.2021.130347
Received 22 June 2021; Received in revised form 17 December 2021; Accepted 31 December 2021
Available online 5 January 2022

approach to determine N_2O emissions (Sun et al., 2017), there are still several challenges in practical applications of mechanistic N_2O models due to their complexity and over-parametrization (Vasilaki et al., 2019). Moreover, full-scale monitoring campaigns of N_2O emissions are necessary for reliable evaluation of N_2O emission models (Gruber et al., 2020; Ribera-Guardia et al., 2019). It should be noted that the number of full-scale practical modelling studies is still limited in the literature (see Table 1).

The discussion on the preferable N_2O model is still ongoing with several extensions and modifications of the original approaches developed recently (Vasilaki et al., 2019). In terms of N_2O production by ammonia oxidizing bacteria (AOB), two categories of N_2O models have been proposed, including single-pathway models and two-pathway models. The single pathway models consider either AOB denitrification or hydroxylamine (NH_2OH) oxidation pathways, while the two-pathway approach has been employed to integrate both N_2O production pathways (Ni and Yuan, 2015). To predict N_2O production by heterotrophic denitrification, the process needs to be modeled as a multiple-step process. Two distinct concepts have been proposed, which are the direct coupling approach represented by the Activated Sludge Model for Nitrogen (ASMN) (Hiatt and Grady, 2008) and the Activated Sludge Model with Indirect Coupling of Electrons (ASM-ICE) (Pan et al., 2013). Inclusion of all major N_2O production pathways results in complex and over parameterized models impairing reliable calibration and validation. Short-term calibration and validation of the models under specific operational conditions limits their accuracy when the system varies significantly. For N_2O production by AOB, the single-pathway models have simplified structures and a fewer number of parameters, which brings convenience to model calibration. The multiple-pathway models have the potential to describe all the N_2O data with different operational conditions, but may require more efforts on model calibration due to a higher number of parameters (Vasilaki et al., 2019). For the single pathway models of AOB reported in the literature, most variable kinetic parameter was, the reduction factor for N_2O production. Regarding the ASM-ICE of heterotrophic denitrifiers, information on the nitrogen reduction kinetics was required for its calibration (Ni and Yuan, 2015).

Models are being calibrated and validated uniquely for a specific WWTP. The conclusions of the modelling study in terms of N_2O pathways and emissions are plant specific. Therefore, continuous improvement and application based on the existing mathematical models are highly recommended (Chen et al., 2020b). Until now, there has been no reported study, addressing confirmation of the existing N_2O models.

In response to this demand, the present study aimed at confirmation of the applicability and universality of an existing N_2O model on another full-scale WWTP. Blomberg et al. (2018) developed Activated Sludge Model No. 3 (ASM3) with an N_2O extension and implemented at the full-scale Viikinmäki WWTP (Finland). In the present study, the same data set was used to evaluate the extended Activated Sludge Model No. 2d (ASM2d-N_2O) validated elsewhere (Zaborowska et al., 2019). Furthermore, both model predictions were compared in terms of a few goodness-of-fits criteria and identification of the major pathways for N_2O production. A rigorous calibration protocol, based on the system engineering approach, was proposed to minimize the number of adjusted parameters without compromising the accuracy of model predictions, specifically in terms of liquid N_2O production and N_2O emission. Ultimately, the model predictions for N_2O emissions resulted in estimation of new EFs and comparison with the empirical EF calculations.

2. Materials and methods

2.1. Characteristics of the WWTP

Viikinmäki WWTP, located in the metropolitan area of Helsinki, is the largest facility in Finland with the population equivalent (PE) over 1 million. Except for the biogas units, the entire plant is built underground. Fig. 1a shows a scheme of one out of nine parallel, identically configured activated sludge lines. The basic annual influent characteristics are given in the Supplementary Information (SI) (Table S1). In 2017, the average influent flow rate was 289,000 m^3/d in which industrial wastewater accounted for approximately 7% of the total influent flow. The average nitrogen load of Viikinmäki WWTP was 16 g N/PE/d and 15.4 g N/PE/d during the calibration and validation period, respectively. The average solids retention time (SRT) of the plant was approximately 9 days during both calibration and validation periods. The air from the process tunnels is conducted outside through an exhaust channel which helps measure gas emissions, including N_2O. In terms of hydrodynamic conditions, the biological reactors are non-ideal flow reactors and are divided into six zones (Z1 to Z6), including two anoxic pre-denitrifying zones (Z1 and Z2), one intermediate (aeration on/off) zone (Z3), and three aerated nitrifying zones (Z4 to Z6). In addition, a mixing zone is located prior to Z1 and a degassing zone follows the last aerobic reactor. Under typical operating, aeration at compartments Z4 to Z6 is run at a DO set point of 3 ± 0.33 g O_2/m^3 using a proportional-integral (PI) control algorithm. Adjustments to the aeration process and control of the intermediate compartments are performed based on ammonium based aeration control (ABAC). Under normal process conditions, three or four of the six compartments are aerated.

2.2. Model development

A computer model of Viikinmäki WWTP (Fig. 1b) was built in GPS-X 8.0 simulation platform (Hydromantis, Canada). This section is dedicated to description of the subsequent steps in model development from experimental data collection through the hydrodynamic and biokinetic sub-models selection.

2.2.1. Experimental data collection

The process monitoring in Viikinmäki WWTP was fully automated and monitored via online analyzers. The collected data included temperature, alkalinity (via ADI, 2045TI analyzer), dissolved oxygen (DO), chemical oxygen demand (COD), mixed liquor suspended solids (MLSS) (via BTG RD-20/10 analyzer), NH_4^+-N (via A-ISE sc analyzer), nitrate (NO_3^--N) (via Nitratax plus analyzer), liquid N_2O concentrations in the first and the last aerobic compartments (via Unisense analyzer) and total N_2O emissions (via Gasmet FTIR analyzer) in the exhaust channel. For model calibration and validation, the same sets of data (two measurement campaigns consisting of 12 days and 5 days) were used as previously described by Blomberg et al. (2018).

2.2.2. Influent characterization model

The influent organic and nitrogen fractions were adopted from the study of Blomberg et al. (2018). The state variables included in the influent characterization model can be found in the SI (Table S2). The influent fractions were determined based on the previous findings according to the online analyzers data and laboratory results collected from the bioreactor inlet. The variation in the soluble organic components was assumed to follow the pattern of the influent NH_4–N, while the variation in the particulate organic matter was assumed to follow the

Table 1
Theoretical (without actual N_2O measurements) and practical (with N_2O measurements) full-scale modelling studies on N_2O production and emission in WWTPs.

Study	Studied WWTP	Size	Configuration	Model used	Software	N_2O emission	Main pathway	Remarks
Therotical study by Domingo-Félez and Smets (2020)	Lynetten, Copenhagen, Denmark	700,000 PE	phase-isolated AS	NDHA (nitrifier nitrification, nitrifier denitrification, heterotrophic denitrification, abiotic production)	MATLAB	EF_{N2O} = 1.2% of the removed NH_4^+-N load (DO = 2.0 mg O_2/L) EF_{N2O} = 0.046k g N_2O/kg NH_4^+-$N_{removed}$ (DO = 0.5 mg O_2/L)	In aerobic conditions, AOB denitrification and DHET denitrification pathway contributions increased at high NO_2^- and low DO concentrations; while the NH_2OH oxidation pathway showed the largest contribution at high DO levels.	Low uncertainty in terms of N_2O emissions achieved, the uncertainty of N_2O emissions during model calibration is commonly overlooked in the literature.
Theoretical study by Massara et al. (2018)	Manresa (Catalonia, Spain)	27,000 m^3/d	A^2O configuration with enhanced biological phosphorus removal (EBPR)	ASM2d-N_2O	MATLAB	EF_{N2O} = 1–11% of the influent TN-load based on different DOs and stripping efficiencies	AOB denitrification was found significant contributor to N_2O emissions.	Low aeration is recommended without disturbing the nitrification process.
Therotical study by Pocquet et al. (2016)			SBR	2-P model, including both pathways for AOB	AQUASIM	EF_{N2O} = 1% of the influent NH_4^+-N load	AOB denitrification pathway was dominant	The model confirmed that the decrease of the NO/N_2O ratio can be explained by an increase of the AOB denitrification pathway to the detriment of the NH_2OH oxidation pathway.
Practical study by Duan et al. (2020)	Adelaide, Australia	60,000 PE	SBR	ASMN	Python	2.08 tonnes of CO_{2e}/year EF_{N2O} = 0.58% of the influent TN-load	NH_2OH oxidation pathway was found dominant	Intermittent aeration with a tight DO (2 mg O_2/L) set point strategy could mitigate the EF levels by 0.2%
Practical study by Zaborowska et al. (2019)	Slupsk WWTP	220,000 PE	A2O configuration	ASM2d-N_2O	GPS-X	EF_{N2O} = 1.6% of the influent TN-load	DHET denitrification was found to be the main pathway of N_2O production under both anoxic and aerobic conditions.	NH_2OH oxidation, AOB denitrification and DHET denitrification pathways included. Strategies to minimize N_2O production via decreasing dissolved oxygen concentration in the aerobic zone and increasing MLR rate.
Practical study by Blomberg et al. (2018)	Viikinmäki WWTP, Helsinki, Finland	1,100,000 PE	A2O configuration	ASM3-N_2O	GPS-X	EF_{N2O} = 1–3 ppm	NH_2OH oxidation pathway was found dominant and the model could describe the N_2O production	NH_2OH oxidation and DHET denitrification pathways were included, AOB denitrification pathway was not included
Practical study by Arnell et al. (2017)	Käppala WWTP, Stockholm, Sweden	500,000 PE	A2O configuration	Benchmark Simulation Model No. 2 with GHG extension (BSM2G)	MATLAB	N_2O emission rate = 30 kg N_2O–N/d	Major N_2O production and emissions occurred in the aerated zones	Plant-wide model plus LCA analysis, full N_2O dynamics was not achieved, NH_2OH oxidation pathway addition to the model is recommended
Practical study by Ni et al. (2015)		50 ML/day	Step-feed full-scale plug-flow activated sludge reactor	ASMN	AQUASIM	EF_{N2O} = 0.69% of the influent TN-load (first step) and EF_{N2O} = 3.5% of the influent TN-load (second step)	The AOB denitrification pathway decreased and the NH_2OH oxidation pathway increased along the path of both steps.	The overall N_2O emission from the step-feed WWTP would be largely mitigated if 30% of the returned sludge were returned to the second step to reduce its biomass nitrogen loading rate

(*continued on next page*)

Table 1 (*continued*)

Study	Studied WWTP	Size	Configuration	Model used	Software	N_2O emission	Main pathway	Remarks
Practical study by Ni et al. (2013)	2 WWTPs in Perth, Australia	4 ML/day and 120 ML/day	Oxidation Ditch and SBR	ASMN	AQUASIM	EF_{N2O} = 0.52% of the influent TN-load	NH_2OH oxidation pathway was found dominant	Only NH_2OH oxidation pathway was included for N_2O production during nitrification

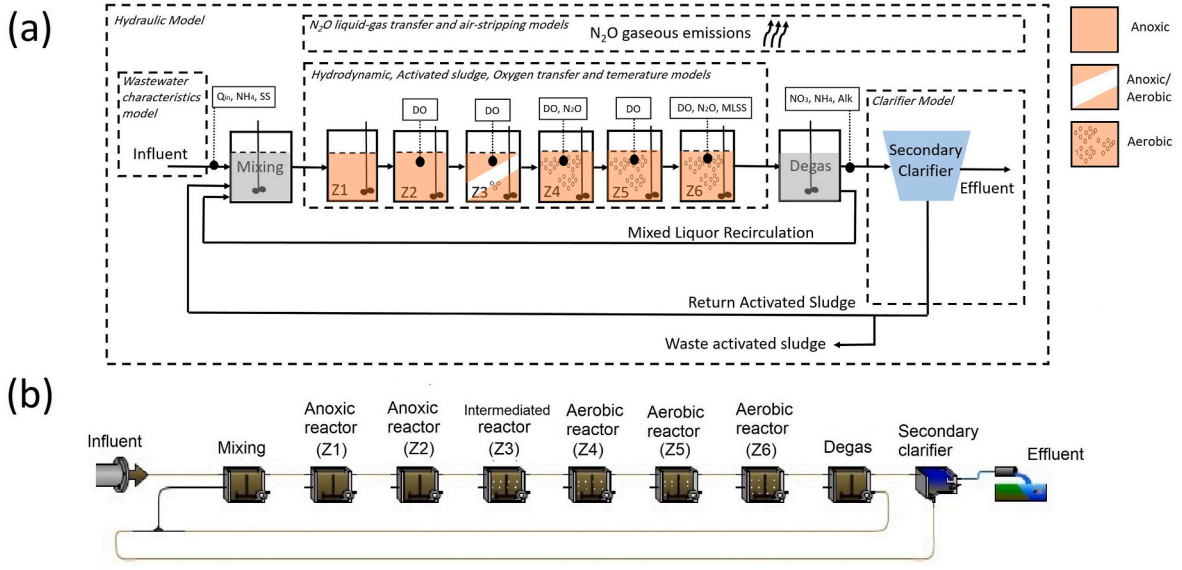

Fig. 1. Configuration of a single activated sludge line at Viikinmäki WWTP: (a) Schematic diagram, (b) GPS-X layout.

pattern of the suspended solids (SS) measurement (Blomberg et al., 2018).

2.2.3. Hydraulic model

The hydraulic model of the bioreactor is based on the modified Ludzack-Ettinger (pre-denitrification) process configuration. The model describes the bioreactor compartments and clarifier dimensions, specific liquid flow rates such as, influent wastewater, mixed liquor recirculation (MLR), return activated sludge (RAS) and mixed liquor flow rates between the bioreactor compartments (Fig. 1).

2.2.4. Hydrodynamic model of the bioreactors

Hydrodynamic models describe the flow patterns inside in the bioreactor compartments. In the absence of tracer measurements, the dispersion coefficient (E_L) can be approximated using the following empirical relationship (Murphy and Boyko, 1970):

$$\frac{E_L}{W^2} = 3.118(q_A)^{3.346} \quad (1)$$

where q_A is the air flow rate per unit reactor volume (s^{-1}) and W is the width of the reactor (m).

With the known E_L, one of the following hydrodynamics models can be selected: a plug-flow reactor (when E_L is close to 0), a completely mixed reactor (E_L greater than 4) or a tank-in-series (TIS), which consists of series of identical completely mixed reactors. The latter model is favorable in the case of deviations from an ideal flow patterns. In order to determine the number of the reactors, the Peclet number (*Pe*) should be calculated using Eq. (2) (Makinia and Zaborowska, 2019):

$$Pe = \frac{uL}{E_L} \text{ in the axial direction} \quad (2)$$

where u is the mean velocity along a reactor (m/s) and L is the reactor's length (m).

Finally, the equivalent number of the completely mixed tanks (N) can be found from the following formula (Laurent et al., 2014):

$$N = \frac{Pe}{2} \quad (3)$$

Potier et al. (2005) proposed an empirical relationship between the actual equivalent number of reactors (N) and the mean hydraulic residence time (HRT) (Fig. S1 in the SI). By estimating the mean HRT, it would be possible to validate number N based on the empirical relationship. Table S3 in the SI provides the data and assumptions used for determining the hydrodynamic model of the reactors.

2.2.5. Biokinetic model of the bioreactor

The biokinetic model was developed as an extension of the International Water Association (IWA) ASM2d (Henze et al., 2000). The ASM2d-N_2O model expanded with the N_2O module was proposed by Zaborowska et al. (2019). In the conceptual model shown in Fig. 2a, three N_2O production pathways were considered, including the final product of autotrophic denitrification mediated by AOB, an intermediate product of NH_2OH oxidation by AOB and denitrifying heterotrophic bacteria (DHET) denitrification. For all the N_2O production pathways, the conceptual model proposed by Lu et al. (2018) was adopted. The model comprised three enzymatic reactions mediated by AOB: (i) NH_4^+ oxidation to N_2O, (ii) NH_4^+ oxidation to nitrite (NO_2^-), (iii) NO_2^- reduction to N_2O, and three sequential reactions mediated by DHET: (i) NO_3^- reduction to NO_2^-, (ii) NO_2^- reduction to N_2O, (iii) N_2O reduction to nitrogen gas (N_2). In the DHET pathway it is important to account for the simultaneous production and consumption of N_2O (Fig. 2b). Further details, including the process rate equations and stoichiometric matrices, are available in the SI (Tables S4 and S5).

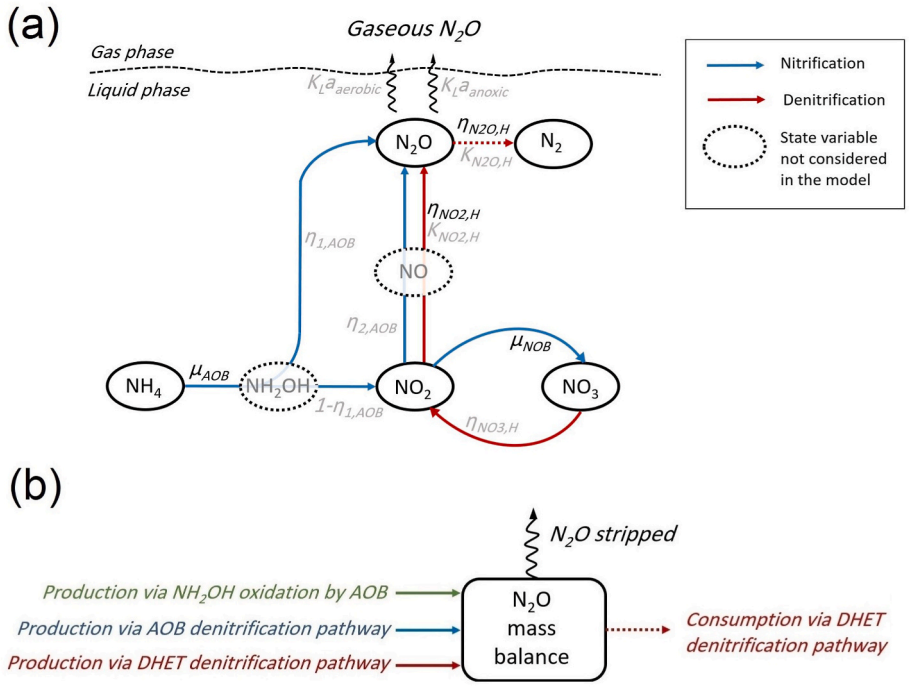

Fig. 2. (a) Mechanisms of N_2O production and consumption (the shown kinetic parameters were adjusted based on the process engineering approach and system engineering approach (only black)), (b) Overall N_2O mass balance in the reactor compartment.

2.2.6. N_2O emission model

Two different N_2O emission models, described in the SI (section S.1) were used separately for the aerated and non-aerated (anoxic) compartments, both developed originally by Schulthess and Gujer (1996). These models were previously applied to predict N_2O emissions in full-scale bioreactors (Baresel et al., 2016). Two methods for the oxygen mass transfer coefficient (K_La) calculations were investigated and compared in this study (see: SI section S.2 for details). The first method comprised K_La estimation based on the oxygen transfer rate (OTR) in the reactor under field conditions. Alternatively, K_La was estimated based on the superficial gas velocity in the reactor (method 2). Finally, in the stripping formulae for the aerobic compartments, $K_La_{\ aerobic}$ was estimated based on the OTR approach (Marques et al., 2016), which induced 10–20% increase in emissions compared to Foley et al. (2010) empirical method. Stripping was incorporated directly in GPS-X whereas in Blomberg et al. (2018) it was calculated using macros. The direct calculation in GPS-X resulted in lower predicted emissions. For the anoxic compartments, the saturation-induced liquid-gas transfer for N_2O

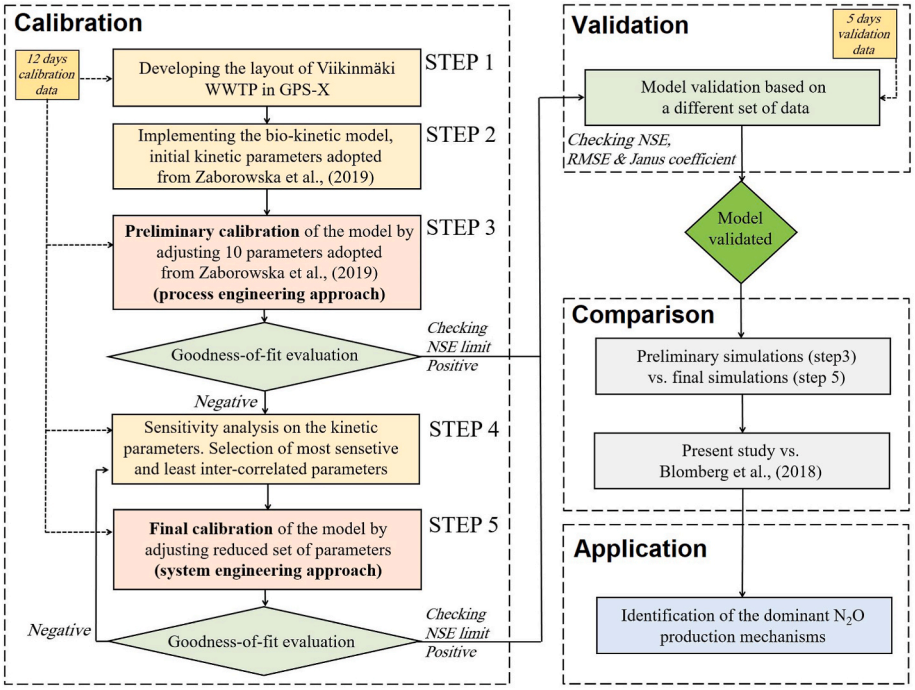

Fig. 3. Systematic step-wise approach to model calibration, validation, comparison and utilization used in the present study.

(K_La_{anoxic}) was assumed at 2 d^{-1} which has widely been used in the literature (Foley et al., 2010; Schulthess and Gujer, 1996; Zaborowska et al., 2019).

The N_2O EF (%) in this study was determined based on the percentage ratio of absolute modeled N_2O emitted from the exhaust channel (kg N_2O) to the total influent TN-load (kg TKN) and calculated as:

$$EF_{N_2O} = \frac{Total\ N_2O\ emissions}{Influent\ TN - load}.100\% \quad (4)$$

Moreover, the N_2O EFs functional units are occasionally reported in the literature based on other ratios, such as, N_2O emitted to the atmosphere to total removed load of nitrogen or NH_4^+-N.

2.3. Model application procedure

The proposed model was calibrated and validated using a systematic step-wise protocol as shown in Fig. 3. In step 1, the process layout of the Viikinmäki WWTP was developed, considering the influent characteristics, and the assumed hydraulic and hydrodynamics models. In step 2, the bio-kinetic model was implemented with the values of kinetic parameters adopted from Zaborowska et al. (2019). In step 3, preliminary calibration was performed based on the process engineering approach adjusting 10 parameters adopted from Zaborowska et al. (2019). The target variables selected for calibration were the concentrations of NH_4^+-N, NO_3^--N, alkalinity, liquid N_2O and gaseous N_2O. Subsequently, the preliminary predictions were evaluated based on the goodness-of-fit criteria. The model results would be approved if both Nash-Sutcliff coefficient (NSE) and root mean square error (RMSE) limit conditions were satisfied, i.e. NSE >0.3 and RMSE <0.5 (the limits adopted from Dai et al. (2017)).

In the case of unsatisfactory results after step 3, the final calibration would be performed based on the system engineering approach. Therefore, local sensitivity analysis (LSA) was carried out in step 4 in order to determine the most influential kinetic parameters. Subsequently, a correlation matrix between the detected influential parameters was determined to eliminate highly correlated parameters and minimize the number of adjusted parameters during the final calibration stage.

In step 5, the reduced set of parameters was estimated using the optimizer utility in GPS-X based on the Nedler-Mead simplex method with the maximum likelihood objective function. If the predictions could not pass the goodness-of-fit criteria, then further calibration should be done by repeating steps 4 and 5 until achieving the satisfactory results.

On the other hand, if the calibrated model passed the test, it would be validated based on another data set. During the validation phase, the model was evaluated based on the same criteria as for calibration and further verified the Janus coefficient. If the model was validated successfully, the final results could be compared with the preliminary results and the previous modelling study performed on Viikinmäki WWTP by Blomberg et al. (2018). The validated model was further applied for N_2O formation pathways analysis.

2.4. LSA and correlation matrix

In order to evaluate model uncertainty and reduce the number of adjusted parameters, LSA was carried out (equation (5)) using a 'one-variable-at-a-time' (OAT) approach by adjusting a perturbation value Δx_j of 10% (±5% of the adjusted value). Different perturbation values, Δx_j, have been reported in the literature ranging from 0.01 to 100% with 10% is being most frequently used in the literature since assuming Δx_j, too small will result in numerical inaccuracies and on the other hand, Δx_j should not be too large because then the nonlinearity of the model will affect the sensitivity calculations (Makinia and Zaborowska, 2019).

$$S_{i,j} = \left| \frac{\Delta y_{i,j}}{y_i} \cdot \frac{x_j}{\Delta x_j} \right| \quad (5)$$

where the $S_{i,j}$ coefficient is the ratio of the percentage change $(\Delta y_{i,j}/y_i)$ in the ith output variable (y_i) to the percentage change $(\Delta x_j/x_j)$ in the jth model parameter (x_j). The kinetic parameters were classified as extremely influential when $S_{i,j} \geq 2$.

The tool used for sensitivity analysis was the GPS-X simulation platform (Hydromantis, Canada) which only supports the LSA. Previously reported studies, e.g. Cosenza et al. (2013), favoured global sensitivity analysis (GSA) over LSA due to the fact that GSA accounts for the interactions between kinetic coefficients simultaneously and examining different parameter values as the combinations of them. To overcome this deficiency of LSA, in the present study, the LSA was combined with the correlation matrix analysis of kinetic parameters in the calibration process. Consequently, the interactions between parameters for each target variable were considered. Furthermore, by developing the correlation matrix of the adjusted parameters, the number of the calibrated parameters were reduced by overlooking the highly correlated pairs of parameters. Zhu et al. (2015) proposed to classify parameters as highly correlated if the correlation coefficient of a pair of parameters is high enough (r > 0.9). Then optimization can be done by adjusting only the most influential kinetic parameter.

2.5. Goodness-of-fit evaluation

In order to evaluate the efficiency of model predictions, appropriate goodness-of-fit measures should be determined in the calibration and validation stage of the modelling study. Verification of goodness-of-fit of the models after calibration was determined using both NSE and RMSE criteria. The mean absolute error (MAE) was examined in addition to the RMSE. Finally, the Janus coefficient was calculated in order to validate the model. Those criteria are described in more detail in the SI (section S.3). Al-Hazmi et al. (2021) compared NSE and RMSE and found a poor correlation among them. Therefore, it was recommended to evaluate the model with more than one criterion to improve evaluation of the prediction accuracy.

2.6. Model comparison

When comparing the two models applied for the Viikinmäki WWTP, the main conceptual difference refers to the approach for nitrogen conversion pathways and intermediates of nitrification and denitrification. In terms of N_2O production by AOB, the present model considers the 3-step two-pathway model, including NH_2OH oxidation and denitrification by AOB (Fig. 2). In contrast, the previous model (Blomberg et al., 2018) neglected the role of autotrophic denitrification. In terms of N_2O production and consumption by heterotrophs, the present model applies 3-step heterotrophic denitrification, while the previous model considered the additional intermediate (NO).

In general, similar emission models were applied as an extension to ASMs in both studies. The identical equations were used for the air-stripped N_2O emission (aerobic compartments) and saturation-induced liquid-gas transfer for N_2O (anoxic compartments). However, for the aerobic compartments, different methods were proposed for calculations of the mass transfer coefficient for oxygen and N_2O. In the present model, following the approach of (Zaborowska et al., 2019), the K_La of oxygen was estimated based on the OTR of the reactor at field conditions to maintain the DO at the desired set-point. In the previous model, K_La was determined from an empirical formula based on the superficial gas velocity in the reactor. Both methods are described in detail in the SI (see: Section S.2).

3. Results and discussion

3.1. Hydrodynamic model

With the known dimensions and average air flow rate in the reactors,

the E_L coefficient, E_L, and *Pe* number, were estimated at 11.7 m^2/s and 16.2, respectively. The hydrodynamics of the reactors was described by the TIS model and the actual number of the equivalent tanks was N = 8. The N number was then validated with the known mean residence time (120 min) and the empirical relationship of Potier et al. (2005) (Fig. S1).

For comparison, in the literature, the equivalent number of tanks ranged from 5 to 20 (Potier et al., 2005). Typical aeration reactors have shown mixing patterns to be equivalent to 3–12 tanks (Makinia and Zaborowska, 2019).

3.2. Evaluation of kinetic parameters

The initial values of kinetic parameters were adopted from Zaborowska et al. (2019) (Table S6 in the SI). The preliminary calibration of those 10 kinetic parameters was carried out based on the process engineering approach. Due to unsatisfactory results (NSE lower than 0 for N_2O liquid concentration), re-calibration (final calibration) was necessary following the systematic protocol (Fig. 3).

3.2.1. LSA

The results of LSA performed on the set of 10 parameters, which were adjusted during preliminary calibration, are shown in Fig. 4. The target variables for sensitivity of each parameter were the concentrations of NH_4^+-N, NO_3^--N, alkalinity, liquid N_2O in the last aerobic compartment and accumulative N_2O emissions from the anoxic and aerobic compartments. The total sensitivity of the parameters, considering all five defined target variables, were determined. The N_2O reduction factor for DHET ($\eta_{N2O,H}$), NO_2^- reduction factor for DHET ($\eta_{NO2,H}$) and AOB maximum specific growth rate (μ_{AOB}) were most influential with the highest S_{ij} = 4.4, 3.3 and 2.5, respectively. Due to the controlled alkalinity at Viikinmäki WWTP, alkalinity was excluded from the further optimization step. Moreover, since the N_2O emission model was highly influenced by the liquid N_2O concentration, the sensitivity coefficients for both targets (liquid and gaseous N_2O) were similar (Fig. 4). For the remaining three target variables (NH_4^+-N, NO_3^--N and liquid N_2O), the set of four most influential parameters, i.e. $\eta_{N2O,H}$, $\eta_{NO2,H}$, μ_{AOB} and maximum specific growth rate of NOB (μ_{NOB}), was used for optimization.

3.2.2. Correlation matrix

Table 2 shows the correlation between pairs of the adjusted parameters. In the present study, there was a high correlation (the absolute value > 0.9) between the NO_3^- and NO_2^- reduction factors for DHET ($\eta_{NO3,H}$ and $\eta_{NO2,H}$). Due to this high correlation and higher influence of $\eta_{NO2,H}$ in comparison with $\eta_{NO3,H}$ (Fig. 4), $\eta_{NO2,H}$ was selected for the final calibration. Furthermore, $\eta_{NO2,H}$ also showed high correlations (0.9) with μ_{NOB} and $\eta_{N2O,H}$. This high correlation refers to NO_2^- related processes during heterotrophic denitrification. While NO_2^- is reduced to N_2O ($\eta_{NO2,H}$), N_2O is subsequently reduced to N_2 gas ($\eta_{N2O,H}$). Both processes, i.e., N_2O production and consumption, occur simultaneously.

Table 2
Correlation matrices of the parameters with the highest overall S_{ij}.

	μ_{AOB}	μ_{NOB}	$\eta_{NO3,H}$	$\eta_{NO2,H}$	$\eta_{N2O,H}$
μ_{AOB}	1				
μ_{NOB}	-0.71	1			
$\eta_{NO3,H}$	-0.68	0.29	1		
$\eta_{NO2,H}$	0.86	-0.90	-0.98	1	
$\eta_{N2O,H}$	-0.36	0.89	0.82	-0.90	1

All the adjusted parameters in this study (Table S6) fall within the range reported in the literature (Zaborowska et al., 2019). The most influential parameters were adjusted during both preliminary and final calibration. The remaining coefficients showed a smaller influence or were highly correlated with one of the most influential parameters. Therefore, $\eta_{NO3,H}$ was excluded during the final calibration. The reduced set of parameters adjusted during final calibration is shown in Fig. 5.

3.3. Simulation results of inorganic nitrogen compounds

Model predictions were first fitted to the measured NH_4^+-N concentrations by adjusting only the most influential parameter (μ_{AOB}). Fig. 6a and c present the model predictions for NH_4^+-N concentrations in the last aerobic compartment (bioreactor effluent) during the final calibration and validation steps. The model predictions were able to follow the NH_4^+-N dynamics in both calibration and validation periods

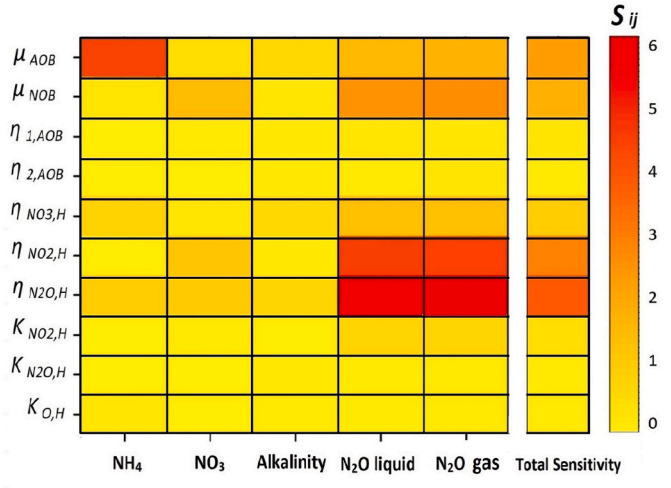

Fig. 4. Sensitivity coefficients of the adjusted parameters during model calibration.

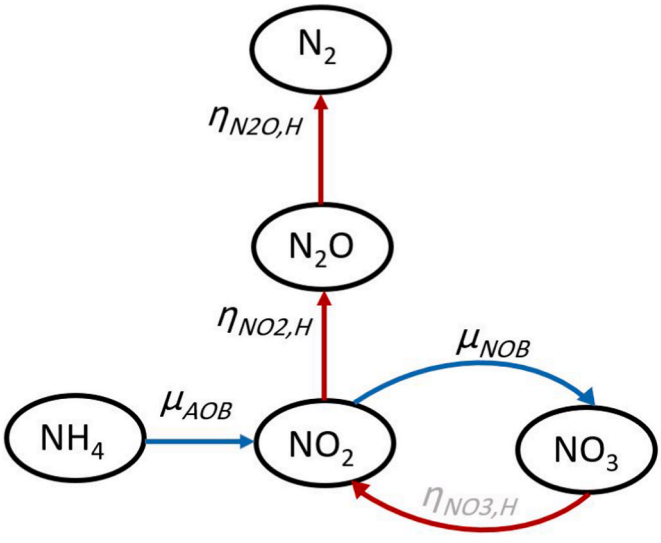

Fig. 5. Kinetic parameters adjusted during final calibration (based on system engineering approach).

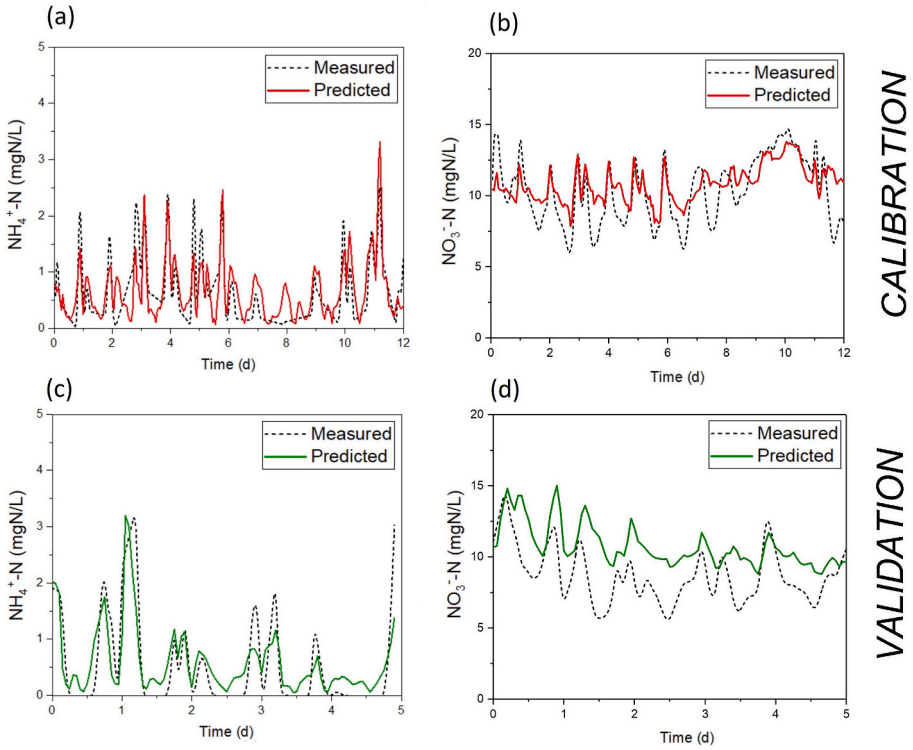

Fig. 6. Predicted (solid line) and measured (dashed line) in the last aerobic compartment (bioreactor effluent): (a) NH_4^+-N and (b) NO_3^-N, concentrations during calibration (red), (c) NH_4^+-N and (d) NO_3^-N, concentrations during validation (green).

Table 3
Goodness-of-fit of the model predictions expressed as the NSE, MAE, RMSE and Janus coefficients.

Parameter	Goodness-of-fit measure	This study		Blomberg et al. (2018) calibration
		Calibration	Validation	
NH_4^+-N	NSE	0.55	0.67	0.28
	RMSE	0.39	0.48	0.50
	MAE	0.30	0.36	0.37
	Janus		1.49	
NO_3^--N	NSE	0.47	0.10	−0.27
	RMSE	1.66	1.87	2.58
	MAE	1.37	1.51	2.08
	Janus		1.12	
Liquid N_2O	NSE	0.35	−0.17	0.26
	RMSE	0.02	0.03	0.03
	MAE	0.02	0.03	0.02
	Janus		1.33	
N_2O emission	NSE	0.33	0.30	−0.95
	RMSE	0.41	0.38	0.70
	MAE	0.31	0.27	0.62
	Janus		0.82	

and passed the goodness-of-fit tests for all the criteria (Table 3).

In the final calibration, μ_{NOB} and $\eta_{NO2,H}$ were adjusted to predict the NO_3^--N concentrations in the last aerobic compartment. Fig. 6b and d show the NO_3^--N predictions in the final calibration and validation steps, respectively. The NO_3^--N concentration dynamics is directly related to denitrification, and thereby, to the variations in the influent organic load. The plant received less organic load during the weekends (days 9–11 during calibration and days 3–5 during validation) which resulted from to a smaller amount of industrial wastewater in that period.

3.4. Simulation results of N_2O production and emission

Fig. 7 presents the dynamic predictions of liquid N_2O and N_2O emissions from the bioreactor. In terms of the liquid N_2O concentration, the model accurately predicted the behavior for the last aerobic zone (Z6), while the predictions were less accurate for the first aerobic zone (Z4). This behavior could be attributed to sudden surges in the liquid N_2O concentration which occurred in the preceding intermediate zone (Z3). Regarding the N_2O emission model, the dynamics of the measured N_2O emissions were captured while maintaining the base level of those emissions in both calibration and validation periods (Fig. 7c and f).

Based on the model predictions of N_2O emission during the calibration period (Fig. 7c), the calculated EF was 0.94% of the influent TN-load. The latest Intergovernmental Panel on Climate Change (IPCC) guidelines recommended the EF of 1.6% of the influent TN-load which is the average of the available literature data (IPCC, 2019). The EF reported by IPCC (2019) is frequently used as an empirical model in the CF assessments to predict the released N_2O from wastewater. The difference of the specific modeled N_2O EF in the present study and the IPCC (2019) empirical EF, would result in approximately 10 kg N_2O/d difference in the predicted emission rate. This means that, in comparison to the mechanistic models, the empirical model would overestimate 952 ton CO_2 equivalent annually.

Foley et al. (2010) reported 1.57% of the removed N-load EF, which is the reference N_2O EF applied in CF calculation tools, e.g. (CFCT, 2014). For comparison, the reported N_2O EFs for other processes are typicallly higher than those for nitrification/denitrification, e.g. 6% of the removed NH_4^+-N load for nitritation (Gustavsson and La Cour Jansen, 2011), and 3% of the removed N-load for partial nitritation/anammox (Kampschreur et al., 2009).

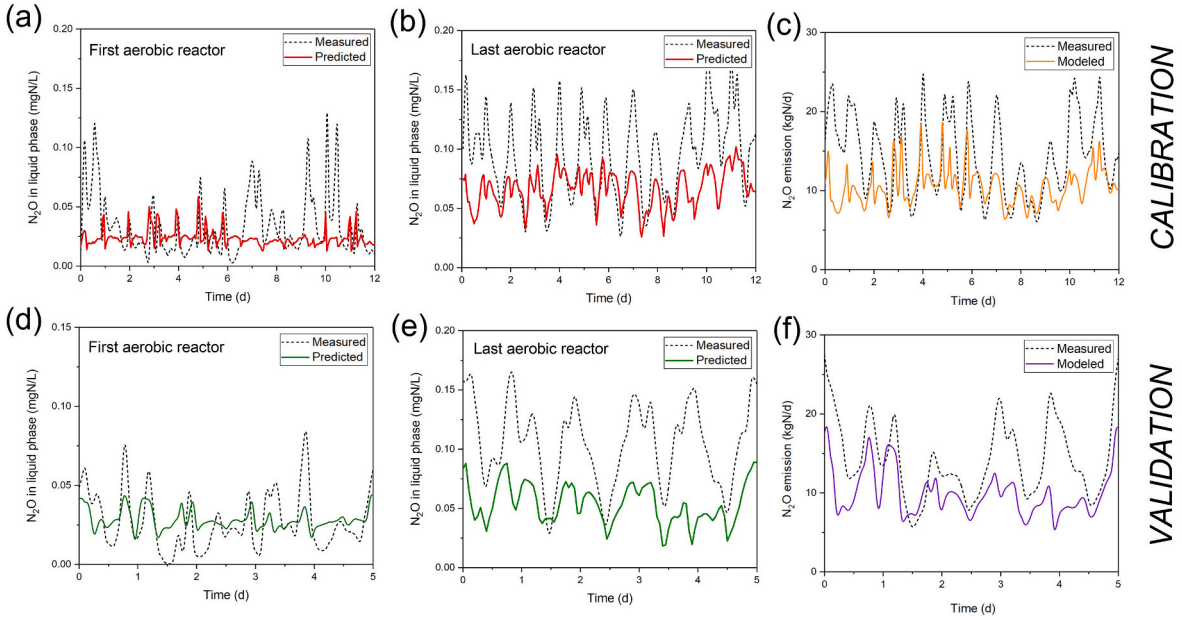

Fig. 7. Predicted (solid line) and measured (dashed line): (a) liquid N_2O concentration in the first aerobic zone (Z4), (b) liquid N_2O concentration in the last aerobic zone (Z6), (c) total N_2O emissions from the biological reactor during calibration; (d) liquid N_2O concentration in Z4, (e) liquid N_2O concentration in Z6, (f) total N_2O emissions from the biological reactor during validation.

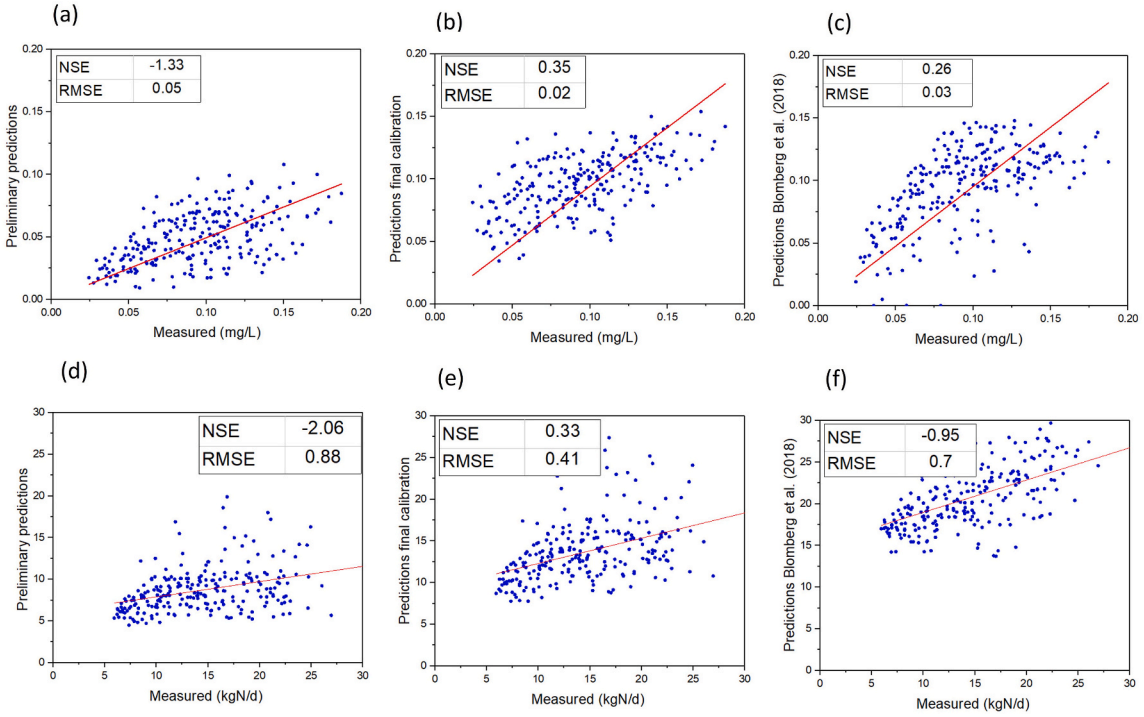

Fig. 8. Model predictions vs. measured data for liquid N_2O concentration in the last aerobic zone (Z6) for: (a) preliminary calibration, (b) final calibration (with the reduced set of parameters), (c) predictions by Blomberg et al. (2018); and model predictions vs. measured data for N_2O gas emissions for: (d) preliminary calibration, (e) final calibration, (f) predictions by Blomberg et al. (2018).

3.5. Comparison of model predictions

3.5.1. Comparison of preliminary and final simulation results

The measured data against model predictions for N_2O liquid concentration in the last aerobic compartment (Z6) and overall N_2O emission are shown in Fig. 8. By optimizing the reduced set of 4 parameters, the model could equally well predict the N_2O emissions, in comparison with the case of adjusting 10 parameters during the preliminary calibration. Fig. 8b shows that the NSE and RMSE coefficients for the liquid N_2O concentration were significantly improved in comparison with the preliminary simulations (Fig. 8a). During the preliminary simulations, the liquid N_2O concentration was underestimated and thus the negative NSE was achieved. This issue was overcome after the final calibration using the system engineering approach when the acceptable goodness-of-fit measure was achieved (NSE = 0.35).

For the N_2O emissions, the model predictions were less accurate.

After the preliminary calibration, the emissions were underestimated which resulted in a negative NSE (Fig. 8d). The stripping model was highly influenced by the liquid N_2O concentration. Therefore, due to the underestimation of liquid N_2O (Fig. 8a), the gaseous emissions were also underestimated. This issue was overcome during the final simulation and the model could better predict the emissions with NSE = 0.33 (Fig. 8e).

3.5.2. Comparison of simulation results with the previous study

The previous modelling study was performed by Blomberg et al. (2018) who applied another model on the same set of data for the calibration and validation periods. The extended ASM3 model was implemented considering NH_2OH oxidation and heterotrophic denitrification pathways. It was reported that the model was able to predict the liquid N_2O concentration accurately, while regarding the emissions, the model was capturing the dynamics of the measured N_2O. However, the base level of the model predictions was higher in comparison with the measured emissions.

Fig. 8b and c show that both modelling studies, i.e. (Blomberg et al., 2018) and the present study, could equally well predict the biological N_2O productions in the liquid phase. In terms of N_2O emissions, the model predictions were improved in this study (Fig. 8e) in comparison with the study of Blomberg et al. (2018) (Fig. 8f) based on the different implementation of stripping as described in section 2.2.6. A similar comparison of the simulation results for other nitrogen compounds is available in the SI (Figs. S2 and S3 for NH_4^+-N and NO_3^--N concentrations, respectively). Furthermore, the OTR method employed, in this study for determination of the K_La of oxygen, enhanced the model predictions of N_2O emissions (see: Fig. S7 in the SI).

Good prediction accuracy was confirmed by the low values of MAE and RMSE obtained for all the targets (Table 3). The MAE values were found very similar for the calibration and validation periods. In order to further evaluate the validated model, the Janus coefficient was calculated for all four analyzed target variables (NH_4^+-N, NO_3^--N, liquid N_2O and N_2O emission). The results showed that the Janus coefficient remained close to 1 in all the cases. This indicates that the model prediction accuracy in the validation period was similar to the calibration period.

3.6. Model application - identifying the dominant N_2O formation pathway

The continuous N_2O production and consumption rates in the anoxic, intermediate and aerobic compartments are presented in Fig. 9. Fig. 9a shows the N_2O consumption and production rates in the last anoxic compartment (Z2). In that compartment, the average N_2O production rate by DHET was 76 mg N/L·d, producing 97% of the total amount of N_2O, while the remaining production was through the AOB denitrification pathway. Simultaneously, over 99% of the produced N_2O was consumed in Z2, leaving the emitted N_2O rate as low as 0.08 mg N/L·d. The model prediction revealed that DHET served as a net N_2O sink in the anoxic compartment.

On the other hand, in the last aerobic compartment (Z6) (Fig. 9b), the average N_2O production rate by DHET was reduced to 13 mg N/L·d (78% share of the total production rate). The relatively high contribution of DHET to N_2O production in the aerobic compartment can be justified by the high biomass concentration of DHET (1295 mg COD/L) vs. AOB (78 mg COD/L). At the same time, the specific rate of NO_2^- heterotrophic reduction to N_2O was estimated at 0.02 d^{-1} in comparison with 0.1 d^{-1} for the AOB nitrification pathway.

In the aerobic compartment, the share of the NH_2OH oxidation pathway in the total N_2O production increased to 20%. As a consequence, the rate of stripped N_2O increased to 1.4 mg N/L·d making it 17 times greater compared to the anoxic compartment. This is clearly demonstrated in Fig. 9c showing the N_2O production and emission rates in the intermediate zone (Z3). During the aeration periods, the share of the NH_2OH oxidation pathway increased and consequently higher amounts of N_2O were emitted. Within all the zones (Fig. 9d), the aerobic

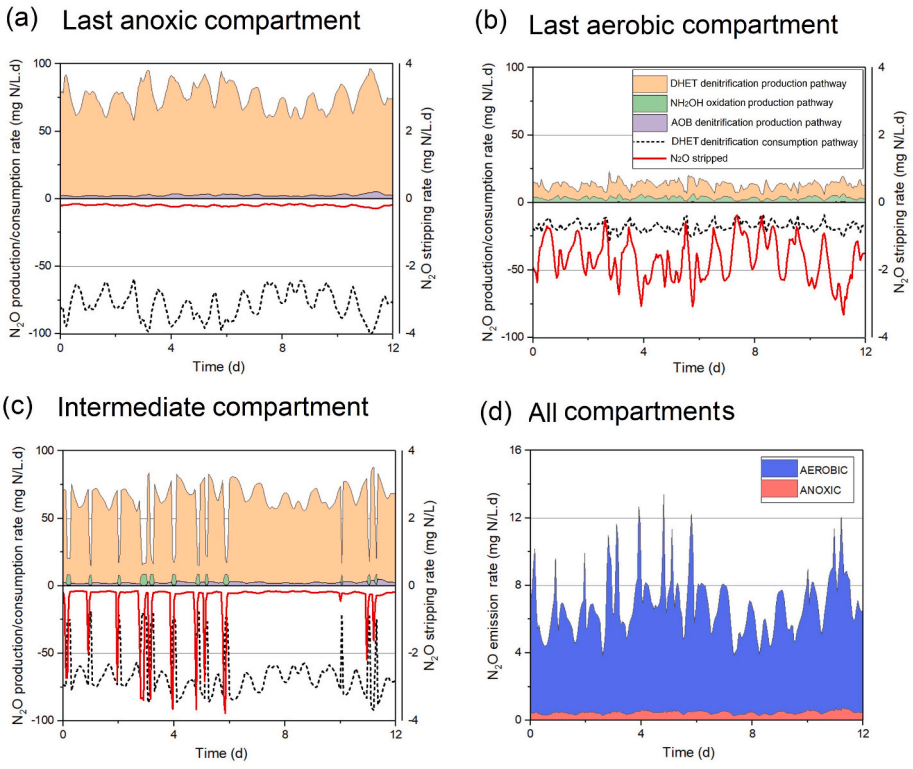

Fig. 9. Model predictions of N_2O production, consumption and emission rates in the selected compartments: (a) last anoxic zone, (b) last aerobic zone, (c) intermediate zone and (d) the N_2O emission rate for the whole bioreactor.

compartments contributed on average to over 93% of the emitted N_2O, while the remaining 7% resulted from the N_2O liquid-gas transfer in the non-aerated zones.

The contribution of the AOB denitrification pathway was found negligible and confirmed the assumption of the previous modelling study at Viikinmäki WWTP by Blomberg et al. (2018). In the N_2O model of Blomberg et al. (2018), the AOB denitrification pathway was excluded. Although that pathway was considered in the present study, the results showed that the share of the AOB denitrification pathway in N_2O production was marginal. In three aerobic compartments, the contribution of that pathway was lower than 2%. The highest share, 3.3% of the total N_2O production rate, was observed in the last anoxic compartment (Fig. 9a). The predictions of N_2O production pathways in the other zones are available in the SI (Fig. S4).

The results of this study are consistent with the modelling study of Sun et al. (2017) in terms of the highly descending order from oxic to anoxic tanks for the total N_2O flux. For the DHET denitrification pathway, both production and consumption rates must be taken into account to reflect the net N_2O production as shown in Fig. 2b. The study of Conthe et al. (2019) confirmed that denitrification could be an effective sink for N_2O, potentially scavenging a fraction of the N_2O produced by NH_4^+ oxidation. Chen et al. (2020c) also pointed out that AOB were N_2O producers, while DHET were both producers and consumers.

The exact triggering operational and environmental conditions that govern N_2O production are still under extensive investigation. Table 1 summarizes the full-scale modelling studies, indicating different dominant pathways of N_2O emission under diverse operational conditions.

The previous modelling study of Blomberg et al. (2018) modeled the N_2O emissions from the aerobic bioreactors (with the average DO ≈ 3 mg O_2/L), including the DHET denitrification and NH_2OH oxidation, and suggested that the latter pathway was the dominant contributor to N_2O emission. The NH_2OH oxidation pathway has been reported in the literature for the environments with higher DO concentrations (Ni et al., 2013; Peng et al., 2015). In contrast, the model of Zaborowska et al. (2019) revealed that the DHET denitrification pathway was predominant in terms of N_2O production in both anoxic and aerobic reactors. In this study, similar to the studies of Domingo-Félez et al. (2017) and Zaborowska et al. (2019), the model showed the highest N_2O production and consumption through the DHET denitrification pathway in both aerated and non-aerated compartments. The actual role of DHET denitrification in N_2O production in the aerobic zones with different DO levels should be investigated in depth in future studies including gene activity measurements. Data from the analyzed gene expression would help identify the key pathways and microbial groups responsible for nitrogen metabolism and N_2O production at specified conditions (Conthe et al., 2019).

Moreover, it was suggested that maintaining the DO levels between 1 and 2 mg O_2/L could minimize the overall N_2O production in the bioreactors. Massara et al. (2018) presented a model including all the biological pathways for N_2O production in a municipal WWTP with the A^2O (anaerobic-anoxic-aerobic) biological configuration. Based on theoretical simulations, it was revealed that with the DO below 1.8 mg O_2/L, the AOB prevailed over NOB and prompted the shift to decreasing NH_4^+ concentration and NO_2–N accumulation. The authors reported that in the DO range of 0.8–1.8 mg O_2/L, the N_2O EF was 10% of the removed NH_4^+-N load, which mainly resulted from the AOB denitrification pathway. Chen et al. (2020b) reported that the DO concentration would need to be maintained above 2 mg O_2/L in aerobic phases to satisfy BNR removal and N_2O mitigation. When the DO concentration is lower than 2 mg O_2/L, the nitrification rate decreases and the intermediates, such as N_2O and NH_2OH, could accumulate in the liquid phase (Li et al., 2020).

3.7. Model limitations

Although mechanistic models are powerful tools to predict N_2O emission from WWTPs, there are limitations found in this comparative study:

- The different findings of the dominant N_2O production pathways have been based on the model predictions only. In order to validate those results, further detailed analysis would be necessary to obtain site specific data on the actual contributions of AOB and DHET which can be obtained by gene activity measurements.
- The data on both liquid N_2O concentration and N_2O emissions in full-scale WWTPs are still limited. Moreover, the developed model only predicted N_2O emissions in the activated sludge reactors, while other elements (e.g. secondary clarifiers) of the WWTP were not taken into account.

4. Conclusions

The direct confirmation of the validated model on another plant was not successful in Viikinmäki WWTP. Therefore, the novel calibration strategy, based on adjusting the most influential and least correlated kinetic coefficients, was developed and successfully applied, which could be exploited in future studies. This allowed to calibrate the model by optimizing only four kinetic parameters. The re-calibrated model accurately predicted the behavior of both liquid N_2O in the bioreactor and N_2O emission in the exhaust channel. The estimated N_2O EF at the studied plant for the calibration period was 0.94% of the influent TN-load. This value falls in the low range of the reported N_2O EFs from the literature with the average of 1.6% of the influent TN-load. The difference between the predicted N_2O EF and the empirical EF would lead to 952 ton CO_2 equivalent reduction of the annual CF of the plant. The model showed the highest N_2O production and consumption rates for DHET denitrification pathway in all the compartments. Furthermore, the DHET denitrification pathway was an effective sink for the produced N_2O, while NH_2OH oxidation was the second contributor to N_2O produced in the aerobic reactors. The contribution of the AOB denitrification pathway was found negligible. In overall, the aerobic zones contributed to over 93% of the emitted N_2O, while the remaining portion resulted from the N_2O liquid-gas transfer in the non-aerated zones.

CRediT authorship contribution statement

Mojtaba Maktabifard: Formal analysis, Methodology, Visualization, Writing – original draft. **Kati Blomberg:** Data curation, Methodology. **Ewa Zaborowska:** Supervision, Methodology, Writing – review & editing. **Anna Mikola:** Conceptualization, Supervision, Writing – review & editing. **Jacek Mąkinia:** Conceptualization, Funding acquisition, Project administration.

Declaration of competing interest

The authors declare that they have no known competing financial interests or personal relationships that could have appeared to influence the work reported in this paper.

Acknowledgment

The authors acknowledge the support provided by InterPhD2 Program funded by European Union/European Social Fund (Project No. POWR.03.02.00-IP.08-00-DOK/16).

Appendix A. Supplementary data

Supplementary data to this article can be found online at https://doi.org/10.1016/j.jclepro.2021.130347.

References

Al-Hazmi, H.E., Lu, X., Majtacz, J., Kowal, P., Xie, L., Makinia, J., 2021. Optimization of the aeration strategies in a deammonification sequencing batch reactor for efficient nitrogen removal and mitigation of N2O production. Environ. Sci. Technol. 55, 1218–1230. https://doi.org/10.1021/acs.est.0c04229.

Arnell, M., Rahmberg, M., Oliveira, F., Jeppsson, U., 2017. Multi-objective performance assessment of wastewater treatment plants combining plant-wide process models and life cycle assessment. J. Water Clim. Chang. 8, 715–729. https://doi.org/10.2166/wcc.2017.179.

Baresel, C., Andersson, S., Yang, J., Andersen, M.H., 2016. Comparison of nitrous oxide (N2O) emissions calculations at a Swedish wastewater treatment plant based on water concentrations versus off-gas concentrations. Adv. Clim. Change Res. 7, 185–191. https://doi.org/10.1016/j.accre.2016.09.001.

Blomberg, K., Kosse, P., Mikola, A., Kuokkanen, A., Fred, T., Heinonen, M., Mulas, M., Lübken, M., Wichern, M., Vahala, R., 2018. Development of an extended ASM3 model for predicting the nitrous oxide emissions in a full-scale wastewater treatment plant. Environ. Sci. Technol. 52, 5803–5811. https://doi.org/10.1021/acs.est.8b00386.

CFCT, 2014. Carbon Footprint Calculation Tool.

Chen, K.H., Wang, H.C., Han, J.L., Liu, W.Z., Cheng, H.Y., Liang, B., Wang, A.J., 2020a. The application of footprints for assessing the sustainability of wastewater treatment plants: a review. J. Clean. Prod. 277, 124053 https://doi.org/10.1016/j.jclepro.2020.124053.

Chen, H., Zeng, L., Wang, D., Zhou, Y., Yang, X., 2020b. Recent advances in nitrous oxide production and mitigation in wastewater treatment. Water Res. 184, 116168 https://doi.org/10.1016/j.watres.2020.116168.

Chen, H., Zeng, L., Wang, D., Zhou, Y., Yang, X., 2020c. Exploring the linkage between free nitrous acid accumulation and nitrous oxide emissions in a novel static/oxic/anoxic process. Bioresour. Technol. 304, 123011 https://doi.org/10.1016/j.biortech.2020.123011.

Conthe, M., Lycus, P., Arntzen, M., Ramos da Silva, A., Frostegård, Å., Bakken, L.R., Kleerebezem, R., van Loosdrecht, M.C.M., 2019. Denitrification as an N2O sink. Water Res. 151, 381–387. https://doi.org/10.1016/j.watres.2018.11.087.

Cosenza, A., Mannina, G., Vanrolleghem, P.A., Neumann, M.B., 2013. Global sensitivity analysis in wastewater applications: a comprehensive comparison of different methods. Environ. Model. Software 49, 40–52. https://doi.org/10.1016/j.envsoft.2013.07.009.

Dai, H., Chen, W., Dai, Z., Li, X., Lu, X., 2017. Efficient model calibration method based on phase experiments for anaerobic–anoxic/nitrifying (A2N) two-sludge process. Environ. Sci. Pollut. Res. 24, 19211–19222. https://doi.org/10.1007/s11356-017-9437-z.

Delre, A., ten Hoeve, M., Scheutz, C., 2019. Site-specific carbon footprints of Scandinavian wastewater treatment plants, using the life cycle assessment approach. J. Clean. Prod. 211, 1001–1014. https://doi.org/10.1016/J.JCLEPRO.2018.11.200.

Domingo-Félez, C., Pellicer-Nàcher, C., Petersen, M.S., Jensen, M.M., Plósz, B.G., Smets, B.F., 2017. Heterotrophs are key contributors to nitrous oxide production in activated sludge under low C-to-N ratios during nitrification—batch experiments and modeling. Biotechnol. Bioeng. 114, 132–140. https://doi.org/10.1002/bit.26062.

Domingo-Félez, C., Smets, B.F., 2020. Modelling N2O dynamics of activated sludge biomass: uncertainty analysis and pathway contributions. Chem. Eng. J. 379, 122311 https://doi.org/10.1016/j.cej.2019.122311.

Duan, H., van den Akker, B., Thwaites, B.J., Peng, L., Herman, C., Pan, Y., Ni, B.J., Watt, S., Yuan, Z., Ye, L., 2020. Mitigating nitrous oxide emissions at a full-scale wastewater treatment plant. Water Res. 185, 116196 https://doi.org/10.1016/j.watres.2020.116196.

Foley, J., de Haas, D., Hartley, K., Lant, P., 2010. Comprehensive life cycle inventories of alternative wastewater treatment systems. Water Res. 44, 1654–1666. https://doi.org/10.1016/J.WATRES.2009.11.031.

Gruber, W., Villez, K., Kipf, M., Wunderlin, P., Siegrist, H., Vogt, L., Joss, A., 2020. N2O emission in full-scale wastewater treatment: proposing a refined monitoring strategy. Sci. Total Environ. 699, 134157 https://doi.org/10.1016/j.scitotenv.2019.134157.

Gustavsson, D.J.I., La Cour Jansen, J., 2011. Dynamics of nitrogen oxides emission from a full-scale sludge liquor treatment plant with nitritation. Water Sci. Technol. 63, 2838–2845. https://doi.org/10.2166/wst.2011.487.

Henze, M., Gujer, W., Mino, T., van Loosdrecht, M., 2000. Activated Sludge Models ASM1, ASM2, ASM2d and ASM3. IWA Publishing.

Hiatt, W.C., Grady, C.P.L., 2008. An updated process model for carbon oxidation, nitrification, and denitrification. Water Environ. Res. 80, 2145–2156. https://doi.org/10.2175/106143008X304776.

IPCC, 2019. Refinement to the 2006 IPCC Guidelines for National Greenhouse Gas Inventories.

Kampschreur, M.J., Temmink, H., Kleerebezem, R., Jetten, M.S.M., van Loosdrecht, M.C.M., 2009. Nitrous oxide emission during wastewater treatment. Water Res. 43, 4093–4103. https://doi.org/10.1016/j.watres.2009.03.001.

Koutsou, O.P., Gatidou, G., Stasinakis, A.S., 2018. Domestic wastewater management in Greece: greenhouse gas emissions estimation at country scale. J. Clean. Prod. 188, 851–859. https://doi.org/10.1016/j.jclepro.2018.04.039.

Laurent, J., Samstag, R.W., Ducoste, J.M., Griborio, A., Nopens, I., Batstone, D.J., Wicks, J.D., Saunders, S., Potier, O., 2014. A protocol for the use of computational fluid dynamics as a supportive tool for wastewater treatment plant modelling. Water Sci. Technol. 70, 1575–1584. https://doi.org/10.2166/wst.2014.425.

Li, L., Ling, Y., Wang, H., Chu, Z., Yan, G., Li, Z., Wu, T., 2020. N2O emission in partial nitritation-anammox process. Chin. Chem. Lett. 31, 28–38. https://doi.org/10.1016/j.cclet.2019.06.035.

Lu, X., Pereira, T.D.S., Al-Hazmi, H.E., Majtacz, J., Zhou, Q., Xie, L., Makinia, J., 2018. Model-based evaluation of N2O production pathways in the anammox-enriched granular sludge cultivated in a sequencing batch reactor. Environ. Sci. Technol. 52, 2800–2809. https://doi.org/10.1021/acs.est.7b05611.

Makinia, J., Zaborowska, E., 2019. In: Mathematical Modelling and Computer Simulation of Activated Sludge Systems, second ed. IWA Publishing.

Mannina, G., Rebouças, T.F., Cosenza, A., Chandran, K., 2019. A plant-wide wastewater treatment plant model for carbon and energy footprint: model application and scenario analysis. J. Clean. Prod. 217, 244–256. https://doi.org/10.1016/j.jclepro.2019.01.255.

Marques, R., Rodriguez-Caballero, A., Oehmen, A., Pijuan, M., 2016. Assessment of online monitoring strategies for measuring N2O emissions from full-scale wastewater treatment systems. Water Res. 99, 171–179. https://doi.org/10.1016/j.watres.2016.04.052.

Massara, T.M., Solís, B., Guisasola, A., Katsou, E., Baeza, J.A., 2018. Development of an ASM2d-N2O model to describe nitrous oxide emissions in municipal WWTPs under dynamic conditions. Chem. Eng. J. 335, 185–196. https://doi.org/10.1016/j.cej.2017.10.119.

Murphy, K.L., Boyko, B.I., 1970. Longitudinal mixing in spiral flow aeration tanks. J. Sanit. Eng. Div. 96, 211–221.

Nayeb, H., Mirabi, M., Motiee, H., Alighardashi, A., Khoshgard, A., 2019. Estimating greenhouse gas emissions from Iran's domestic wastewater sector and modeling the emission scenarios by 2030. J. Clean. Prod. 236, 117673 https://doi.org/10.1016/j.jclepro.2019.117673.

Ni, B.J., Yuan, Z., 2015. Recent advances in mathematical modeling of nitrous oxides emissions from wastewater treatment processes. Water Res. https://doi.org/10.1016/j.watres.2015.09.049.

Ni, B.J., Pan, Y., Van Den Akker, B., Ye, L., Yuan, Z., 2015. Full-scale modeling explaining large spatial variations of nitrous oxide fluxes in a step-feed plug-flow wastewater treatment reactor. Environ. Sci. Technol. 49, 9176–9184. https://doi.org/10.1021/acs.est.5b02038.

Ni, B.J., Ye, L., Law, Y., Byers, C., Yuan, Z., 2013. Mathematical modeling of nitrous oxide (N2O) emissions from full-scale wastewater treatment plants. Environ. Sci. Technol. 47, 7795–7803. https://doi.org/10.1021/es4005398.

Pan, Y., Ni, B.J., Yuan, Z., 2013. Modeling electron competition among nitrogen oxides reduction and N 2O accumulation in denitrification. Environ. Sci. Technol. 47, 11083–11091. https://doi.org/10.1021/es402348n.

Peng, L., Ni, B.J., Ye, L., Yuan, Z., 2015. Selection of mathematical models for N2O production by ammonia oxidizing bacteria under varying dissolved oxygen and nitrite concentrations. Chem. Eng. J. 281, 661–668. https://doi.org/10.1016/j.cej.2015.07.015.

Pocquet, M., Wu, Z., Queinnec, I., 2016. A two pathway model for N 2 O emissions by ammonium oxidizing bacteria supported by the NO/N 2. O variation 88, 948–959. https://doi.org/10.1016/j.watres.2015.11.029.

Potier, O., Leclerc, J.P., Pons, M.N., 2005. Influence of geometrical and operational parameters on the axial dispersion in an aerated channel reactor. Water Res. 39, 4454–4462. https://doi.org/10.1016/j.watres.2005.08.024.

Ribera-Guardia, A., Bosch, L., Corominas, L., Pijuan, M., 2019. Nitrous oxide and methane emissions from a plug-flow full-scale bioreactor and assessment of its carbon footprint. J. Clean. Prod. 212, 162–172. https://doi.org/10.1016/j.jclepro.2018.11.286.

Schulthess, R.V., Gujer, W., 1996. Release of nitrous oxide (N2O) from denitrifying activated sludge: verification and application of a mathematical model. Water Res. 30, 521–530. https://doi.org/10.1016/0043-1354(95)00204-9.

Sun, S., Bao, Z., Li, R., Sun, D., Geng, H., Huang, X., Lin, J., Zhang, P., Ma, R., Fang, L., Zhang, X., Zhao, X., 2017. Reduction and prediction of N2O emission from an Anoxic/Oxic wastewater treatment plant upon DO control and model simulation. Bioresour. Technol. 244, 800–809. https://doi.org/10.1016/J.BIORTECH.2017.08.054.

Vasilaki, V., Massara, T.M., Stanchev, P., Fatone, F., Katsou, E., 2019. A decade of nitrous oxide (N2O) monitoring in full-scale wastewater treatment processes: a critical review. Water Res. https://doi.org/10.1016/j.watres.2019.04.022.

Zaborowska, E., Lu, X., Makinia, J., 2019. Strategies for mitigating nitrous oxide production and decreasing the carbon footprint of a full-scale combined nitrogen and phosphorus removal activated sludge system. Water Res. 162, 53–63. https://doi.org/10.1016/j.watres.2019.06.057.

Zhu, A., Guo, J., Ni, B.J., Wang, S., Yang, Q., Peng, Y., 2015. A novel protocol for model calibration in biological wastewater treatment. Sci. Rep. 5, 29–32. https://doi.org/10.1038/srep08493.